

Supporting Information

Assembly of Carbon Nanotubes and Alkylated-Fullerenes: Nanocarbon-Hybrid towards Photovoltaic Applications

Yanfei Shen,^{*a} Juan Sebastián Reparaz,^b Markus Raphael Wagner,^b Axel Hoffmann,^b Christian Thomsen,^b Jeong-O Lee,^c Sebastian Heeg,^d Benjamin Hatting,^d Stephanie Reich,^d Akinori Saeki,^e Shu Seki,^e Kaname Yoshida,^f Sukumaran Santhosh Babu,^a Helmuth Möhwald^g and Takashi Nakanishi^{*a}

^a *National Institute for Materials Science (NIMS), 1-2-1 Sengen, Tsukuba 305-0047, Japan*

^b *Technische Universität Berlin, 10623 Berlin, Germany*

^c *Korea Research Institute of Chemical Technology, Daejeon 305-343 Korea*

^d *Freie Universität Berlin, 14195 Berlin, Germany*

^e *Graduate School of Engineering, Osaka University, Osaka, Japan*

^f *Institute for Chemical Science, Kyoto University, Japan*

^g *Max Planck Institute of Colloids and Interfaces, 14424 Potsdam, Germany*

e-mails: SHEN.Yanfei@nims.go.jp (Dr. Yanfei Shen);
NAKANISHI.Takashi@nims.go.jp (Dr. Takashi Nakanishi)

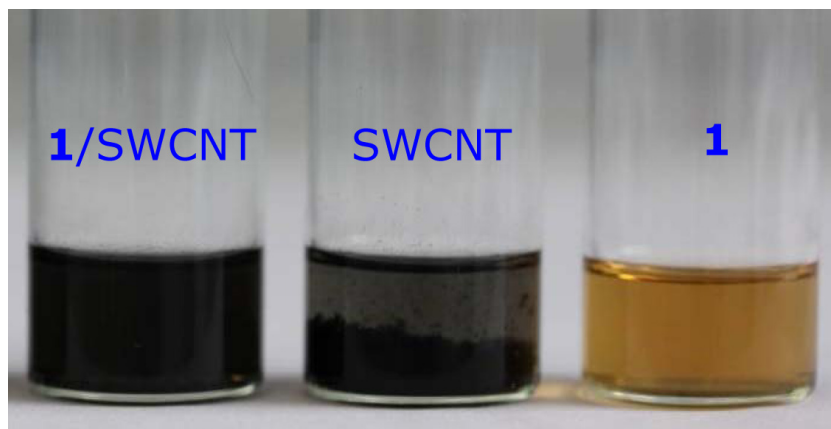


Figure S1. Photos of **1**-SWCNT, SWCNT and **1** in CHCl_3 , demonstrating that SWCNT can be well dispersed in CHCl_3 by **1**.

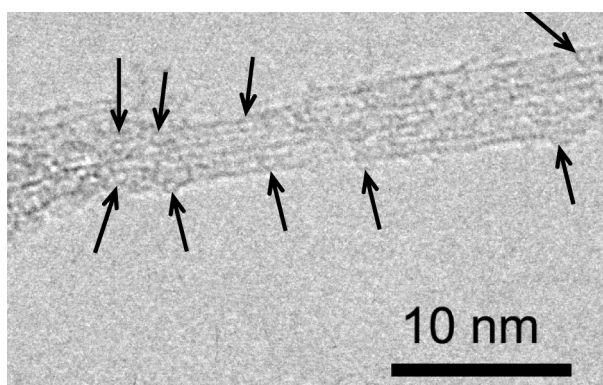


Figure S2. HR-TEM of **1**-SWCNT assembly. The TEM sample was treated with THF to remove excess unbound **1**, for keeping better visualization of debundled SWCNT.

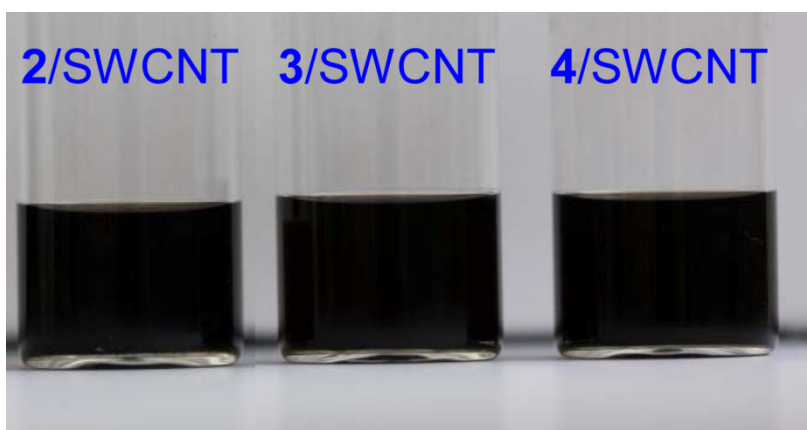


Figure S3. Photos of SWCNT with C_{60} derivatives **2-4** in THF solution, showing that SWCNT can also be dispersed with the aid of other alkylated- C_{60} with different alkyl chain length or different number of alkyl chains.

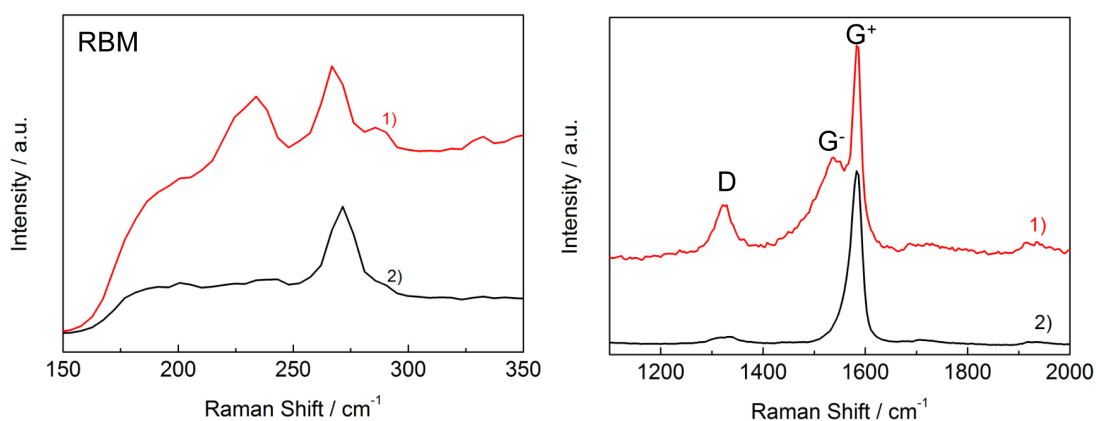


Figure S4. Raman spectra of **1**-SWCNT in THF (1) and SWCNT in SDS aqueous solution (2) by the laser excitations at 532 nm.

The enhanced D band in the spectrum of **1**-SWCNT could be an indication that sonication during the sample preparation may cause shortened carbon nanotubes or defects along the sidewall. In addition, compared to the spectrum of SWCNT in SDS aqueous solution, an additional band at 233 cm^{-1} in radical breathing mode (RBM) region appeared in the spectrum of **1**-SWCNT, which can be assigned to metallic nanotubes. This is consistent with the appearance of G^- band.^[1] In general, SDS has no selectivity for dispersing SWCNT in aqueous solution. Interestingly, our C_{60} derivatives have selective solubilization of SWCNT, as we can find that metallic SWCNT were evidently enriched from the Raman spectra. The separation of metallic nanotubes and semiconducting ones has been reported, which greatly pave the practical applications of SWCNT when only metallic or semiconducting tubes are needed.^[2] More details need further investigation in our future work.

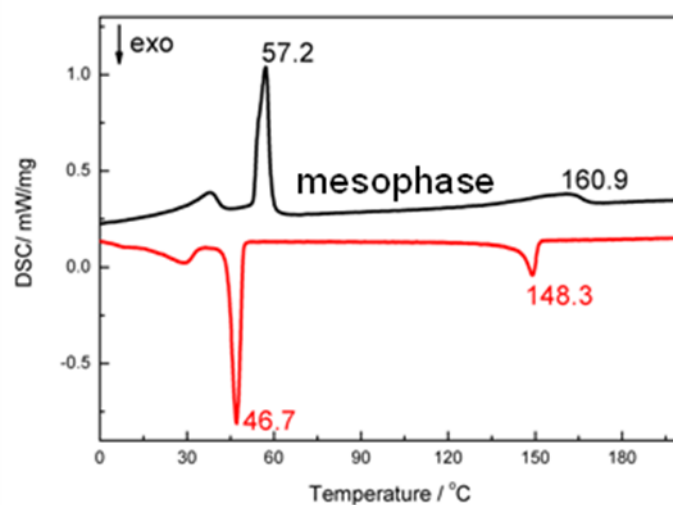


Figure S5. DSC thermograms for the first heating and cooling of **1**-SWCNT assembly.

Compared with the DSC data of **1**, both the phase transition temperature and melting point decreased obviously.^[3] The phase transition temperature and melting point will not change if there is apparent phase separation between SWCNT and **1**. Therefore, one can conclude that SWCNT uniformly dispersed in **1**. Consequently, this DSC data also provided additional proof of the strong interaction between **1** and SWCNT.

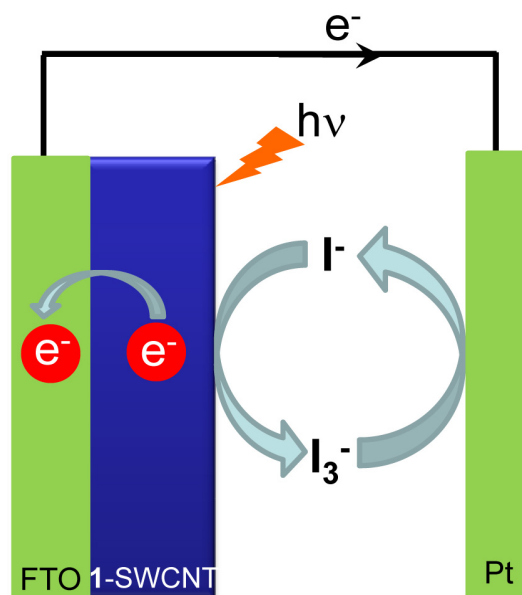


Figure S6. Schematic photoelectrochemical cell configuration.

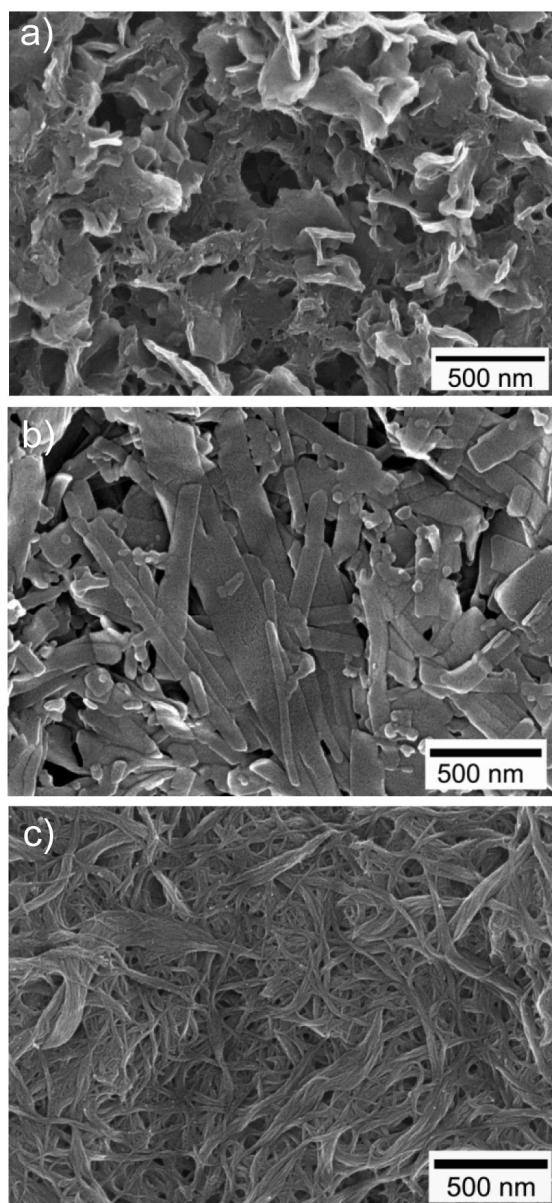


Figure S7. SEM images of a) **1**-SWCNT, b) **1** and c) SWCNT on FTO.

The aggregation of **1**-SWCNT and **1** for photoelectrochemical measurements were obtained by rapid injection equivalent volume of methanol to certain amount of THF solution of **1**-SWCNT and **1** (concentration of **1** is 0.2 mM). Afterwards, these aggregation were cast onto FTO for further photoelectrochemical measurements. SWCNT/FTO was prepared by casting from SWCNT/SDS solution. The clustering behavior of **1**-SWCNT and **1** looks not similar. The former forms hierarchical nanostructure with SWCNT covered by **1** and aggregation of **1**, while the later forms mixture of nanoparticles and nanobelt. All these films have similar thickness of 3~4 μm , which were evaluated using Surf Corder ET 200.

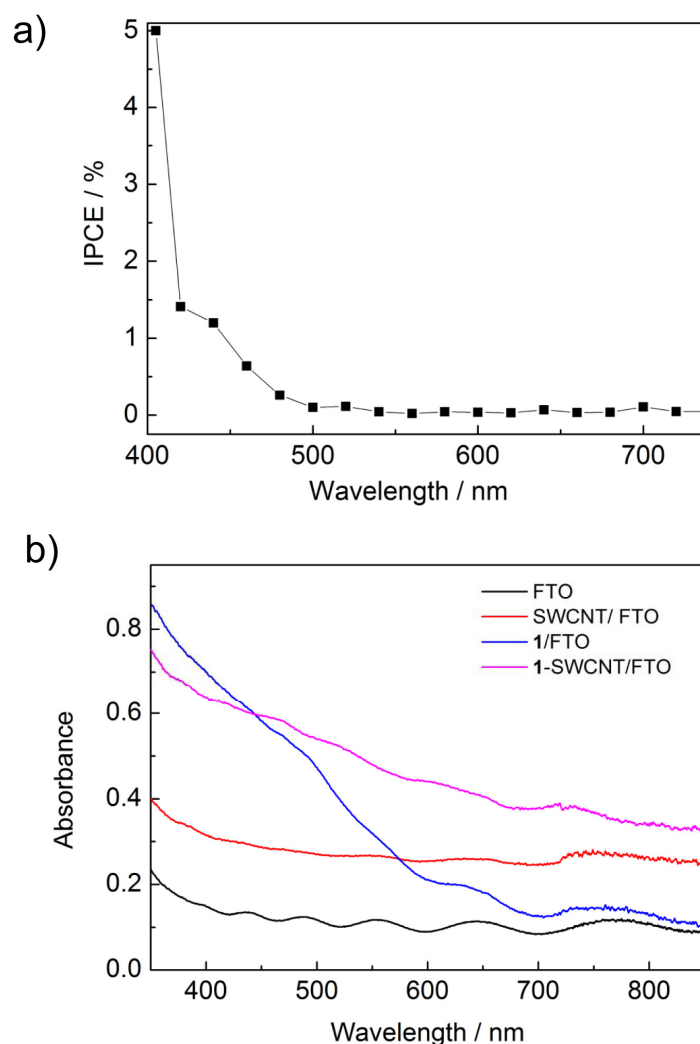


Figure S8. a) Photocurrent action spectrum of **1**-SWCNT/FTO; b) UV-Vis-NIR spectra of films of **1**-SWCNT/FTO, **1**/FTO, SWCNT/FTO and FTO itself.

UV-Vis-NIR spectra were obtained with Shimadzu UV-3600 spectrophotometer equipped with an integrating sphere. The IPCE value reaches close to zero at $\lambda = 550-740$ nm, which does not match the absorption of **1**-SWCNT/FTO. It should be noted that the absorbance of **1**-SWCNT at $\lambda = 550-740$ nm mainly comes from SWCNT. These results show that the contribution by the excitation of **1** is dominant for the photocurrent generation while the one from SWCNT is minor, which is consistent with the photocurrent enhancement of **1**-SWCNT/FTO compared with that of SWCNT/FTO in Fig. 3.

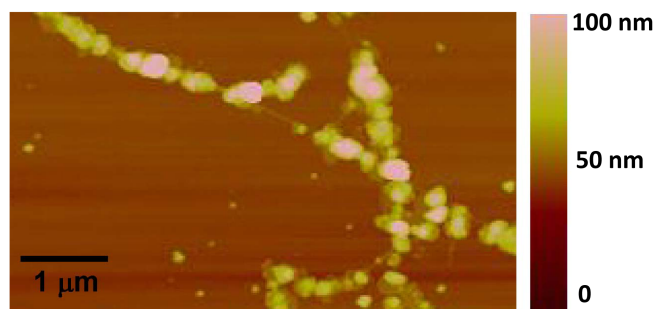


Figure S9. AFM image of **1**-decorated SWCNT FET device, where **1** forms 40 to 120 nm sized clusters on SWCNT surfaces. The size of **1** clusters along SWCNT is estimated from the height information of the image.

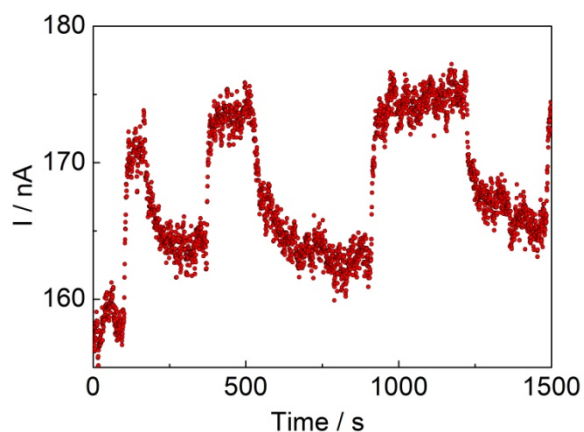


Figure S10. Photoresponse of **1**-decorated SWCNT-FET to the illumination cycle of an Osram lamp (12 V, 100 W) with a bias voltage at 100 mV and a gate bias at 0 V.

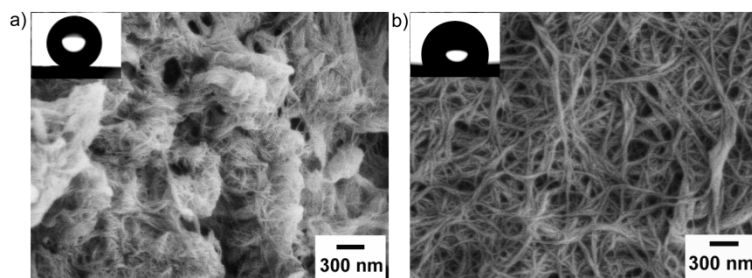


Figure S11. SEM images of 1-SWCNT a) and SWCNT b) deposited onto a glass slide from THF solution after ultrasound treatment of the mixture of **1** and SWCNT about 10 min, inset: photos of a water droplet on the 1-SWCNT or SWCNT surface, the static water contact angles are 154° and 104°, respectively.

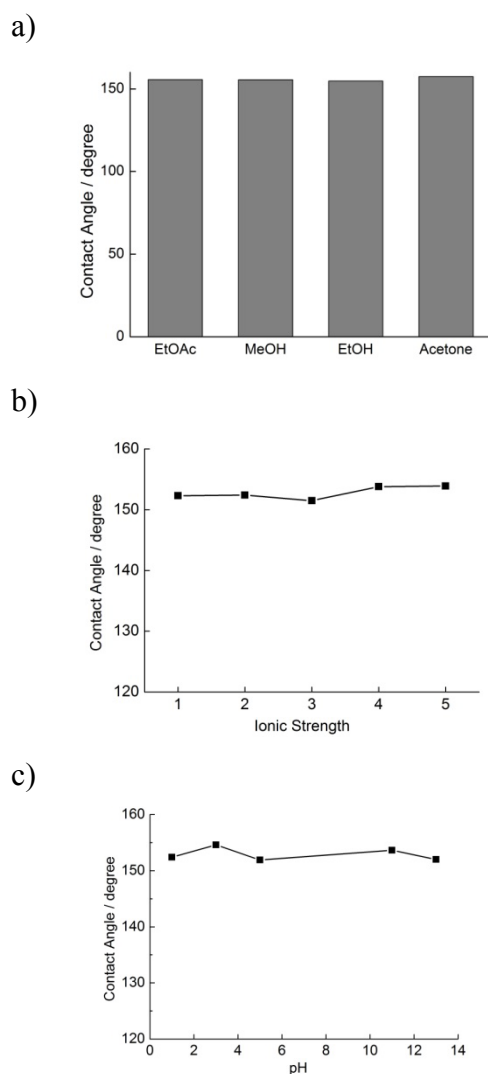
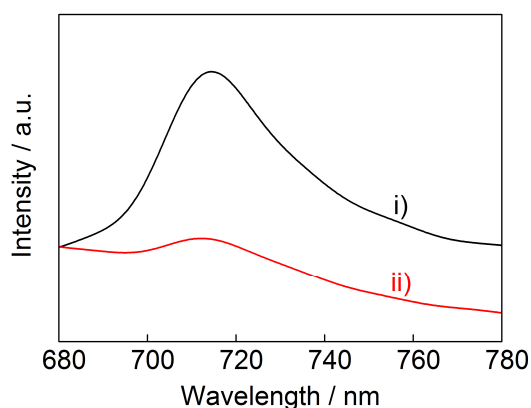


Figure S12. Water repellent property of 1-SWCNT surface for evaluations in the resistivity to a) solvent, b) ionic strength and c) pH.

The **1**-SWCNT assembly provides an anti-wetting surface, which is essential for practical applications. The SEM image (Fig. S8) shows that the surface of SWCNT is fully coated with the assembled **1** showing different thickness and roughness in nano and micrometer scale. The hydrophobicity of **1** and the surface roughness in both nano- and micrometer scale provided by SWCNT are expected to have a water repellent feature, which was proved by the static water contact angle (CA) measurement. As shown in the inset of Fig. S9a, the surface of the **1**-SWCNT assembly features superhydrophobicity with a CA of 154°. In contrast, the surface of the SWCNT film coating without **1** shows lower roughness with a CA of 104° (Fig. S9b), which is hydrophobic but not in the range of superhydrophobicity. The superhydrophobic films of **1**-SWCNT possess high durability under a variety of environmental conditions, such as various acidity, basicity, ionic strength and polar solvents (Fig. S10). Creating superhydrophobicity of nanocarbon materials would be beneficial for their applications in optoelectronic devices to prevent the effect of water on the performance of devices which require high durability in environmental conditions. Although lots of research achievements have aimed at construction of superhydrophobic materials composed of nanocarbons such as SWCNT^[4] and C₆₀ derivatives,^[5] so far, there is no study trying to go beyond such a surface morphology control, e.g., to explore their optoelectronic features together with the wettability control based on the same nanocarbon components. Herein, the easy fabrication and high stability of the superhydrophobic **1**-SWCNT assembly would broaden the scope for potential applications of nanocarbon hybrid materials.

a)



b)

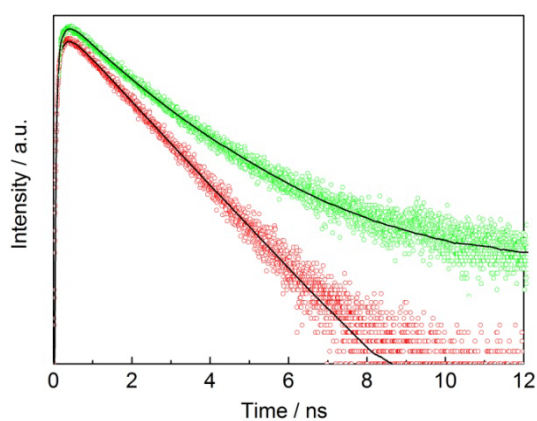


Figure S13. a) Steady-state fluorescence spectra of **1** (curve *i*) and **1**-SWCNT (curve *ii*) in THF; b) time-resolved fluorescence spectra of **1** (red) (at 715 nm) and **1**-SWCNT (green) (at 712 nm) and their fitting curves (black) in THF, $\lambda_{ex} = 400$ nm.

The fluorescence decay of **1** in THF was fitted with a single-exponential function and resulted in a lifetime of 1320 ps at 715 nm. In the **1**-SWCNT THF solution, a biexponential decay function was observed with lifetimes of 950 ps (55%) and 2000 ps (45%), where the shorter component reflects an energy transfer process between the two complexes and the longer one is attributed to recombination of the first excited state of **1**.

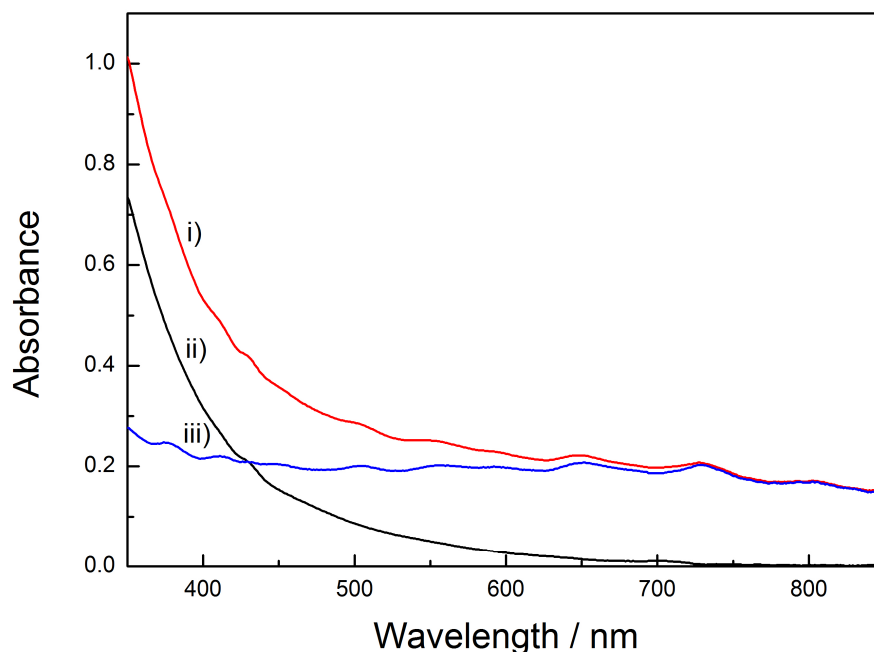


Figure S14. UV-Vis-NIR spectra of diluted THF solution of i) **1**-SWCNT, ii) **1** and iii) difference spectrum by subtracting curve ii) from curve i). The concentration of **1** is about 0.03 mM.

The UV-VisNIR spectra show that at 355 nm, C₆₀ moiety was mainly excited in **1**-SWCNT in TRMC measurements.

References

- [1] Q. Cheng, S. Debnath, E. Gregan, H. J. Byrne, *Appl. Phys. A*, 2011, **102**, 309.
- [2] S. Campidelli, M. Meneghetti and M. Prato, *Small*, 2007, **3**, 1672-1676
- [3] T. Nakanishi, Y. Shen, J. Wang, S. Yagai, M. Funahashi, T. Kato, P. Fernandes, H. Möhwald and D. G. Kurth, *J. Am. Chem. Soc.*, 2008, **130**, 9236.
- [4] S. Srinivasan, V. K. Praveen, R. Philip, A. Ajayaghosh, *Angew. Chem. Int. Ed.*, 2008, **47**, 5750.
- [5] J. Wang, Y. Shen, S. Kessel, P. Fernandes, K. Yoshida, S. Yagai, D. G. Kurth, H. Möhwald, T. Nakanishi, *Angew. Chem. Int. Ed.*, 2009, **48**, 2166.